Bi_2O_3 Nanoparticle Clusters: *Reversible* Agglomeration Revealed by Imaging and Nano-Impact Experiments

T. R. Bartlett[a], S. V. Sokolov[a], J. Holter[b], N. Young[b] and R. G. Compton[a]*

Abstract: Solutions of uncapped, weakly charged Bi_2O_3 nanoparticles are studied in aqueous solution. Nanoparticle tracking analysis reveals the particles to be agglomerated. In contrast electrochemical detection via the nano-impacts technique shows almost exclusive detection of monomeric nanoparticles. Comparison of the two techniques allows the conclusion to be drawn that the agglomeration/deagglomeration of the nanoparticles is *reversible*. A minimum rate constant for the deagglomeration process is estimated.

Introduction

The detection and quantitative sizing of single nanoparticles (NPs) is a growing area of research [1]. In the new nano-impacts technique suspended NPs collide with an electrode held at a suitably reductive or oxidative potential resulting in the complete electrolysis of the incident particle[2]. Measurement of the charge passed during each electrolysis event can be directly related to the size of the impacted NP and provides sizing information of each individual particle. The range of materials characterised voltammetrically by electrolytic nano-impacts is expanding and now covers a range of metallic[2-3], metal oxide[4], metal halide[5], organic[6], polymeric particles[7] and even biological entities such as liposomes[8], bacteria[9] and viruses[10].

An important topic of research for suspended NPs is that of inter-particle interactions and the processes of agglomeration and aggregation[11]. The relative extent of these processes in NP systems is important across the field of nanotechnology affecting NP reactivity[12] and distribution in the environment[13]. The IUPAC definition of agglomeration is a *reversible* process whereby dispersed particles are held together by weak physical interactions leading to phase separation by the formation of precipitates of larger than colloidal size[14]. Aggregation is defined as an *irreversible* process in which particles are strongly bonded together to form clusters. A model for the equilibrated *reversible* agglomeration of NPs has recently been derived[15] permitting the distribution of agglomerates to be predicted assuming an entropy of mixing only model. This model takes the entropy of mixing as the important driving force for the resultant particle size distribution explaining why often, despite weakly repulsive forces between the particles, agglomeration is nevertheless observed.

Agglomerated NPs have been previously observed by nano-impacts[16]. Citrate-capped Ag NPs impacts were measured and directly compared to NTA, with the resultant distribution for both cases showing excellent agreement, matching the size and distribution of the clusters. Here monomeric, dimeric, trimeric etc. NPs were detected in their clustered forms at the electrode and thus the agglomeration of NPs could be directly observed. This requires the kinetics of agglomeration/deagglomeration to be slow with respect to the voltammetric timescale ($\sim r^2/D$, where r is the electrode size and D is the diffusion coefficient of the NP). The *reversible but slow* nature of this agglomeration/deagglomeration behaviour was later confirmed by nano-impact experiments[17]. The addition of a magnetic field on super-paramagnetic Fe_3O_4 NPs has also been shown to promote agglomeration, with dimeric and trimeric clusters detected by nano-impacts[18]. In cases such as these, the inter-particle interactions are studied by forcing agglomeration/deagglomeration by applying external forces and then impacting the NPs. In these examples the nano-impacts method quantitatively detects dimers and trimers as well as monomers. Given that the latter diffuses to the electrode faster than the larger species this requires the rate of agglomeration/deagglomeration to be slow. It is interesting and technologically important to ask the question if there are cases where the agglomeration/deagglomeration kinetics are “fast” enough to outrun experimental timescales.

The aim of this paper is to identify such rapid agglomeration/deagglomeration processes through the comparison of NTA and nano-impact experiments of uncapped Bi_2O_3 NPs. NTA provides information of the equilibrated agglomerate size distribution, however cannot directly provide information on the speed of agglomeration/deagglomeration. If the deagglomeration rate is faster than the diffusion of the agglomerates to the electrode surface, nano-impacts may be able to resolve these effects. Due to the equilibrium inherent in agglomeration, some monomeric form must be present in suspension. Electrolysis of these monomers at the electrode surface would drive the equilibrium towards the release of monomer and hence drive rapid deagglomeration of the particle. Electrolysis of the impacting NPs would therefore act as a voltammetric perturbation of the system whilst simultaneously detecting the monomers formed. This approach accesses much faster deagglomeration kinetics than conventional sonication or bubbling methods [19] and should allow resolution of rapid agglomeration/deagglomeration effects through exclusive or near exclusive detection of the monomeric form. The identity of the impacting aggregate can additionally be inferred indirectly by imaging of the nano-deposits remaining on the surface after impact [20].

[a] Mr. T. R. Bartlett, Mr. S. V. Sokolov, Prof. Dr. R. G. Compton
Department of Chemistry
Oxford University
Physical and Theoretical Chemistry Laboratory, South Parks Road, Oxford, OX1 3QZ, UK.
E-mail: richard.compton@chem.ox.ac.uk
[b] Mrs. J. Holter, Dr. N. Young
Department of Materials
University of Oxford
Parks Road, Oxford, OX1 3PH, UK.

Results and Discussion

First, the voltammetric response of Bi_2O_3 NPs is studied by use of drop-cast modified glassy carbone (GC) macroelectrodes to establish the potentials required for nano-impact experiments. Next, nano-impact experiments are conducted at a carbon microelectrode across a range of reductive potentials and quantitative sizing achieved. Finally, the results gained from electrochemical analysis of the NPs is critically compared with results gained from NTA and SEM imaging discussed in terms of agglomeration/deagglomeration.

A GC macroelectrode was modified with 0.69 nmoles of Bi_2O_3 NPs and stripped voltammetrically in 0.10 M NaOH as seen in Fig 1 (top). A clear reductive peak is observed at -1.33 V vs MSE consistent with the known $3e^-$ reduction of Bi_2O_3[21]:

C1: $$Bi_2O_3 + 2OH^- \rightleftharpoons 2BiO_2^- + H_2O$$
$$BiO_2^- + 2H_2O + 3e^- \rightarrow Bi + 4OH^-$$

A shoulder at -1.45 V vs MSE is also apparent and is attributed to the $6e^-$ reduction of Bi_2O_3[21]:

C2: $$Bi_2O_3 + 3H_2O + 6e^- \rightarrow 2Bi + 6OH^-$$

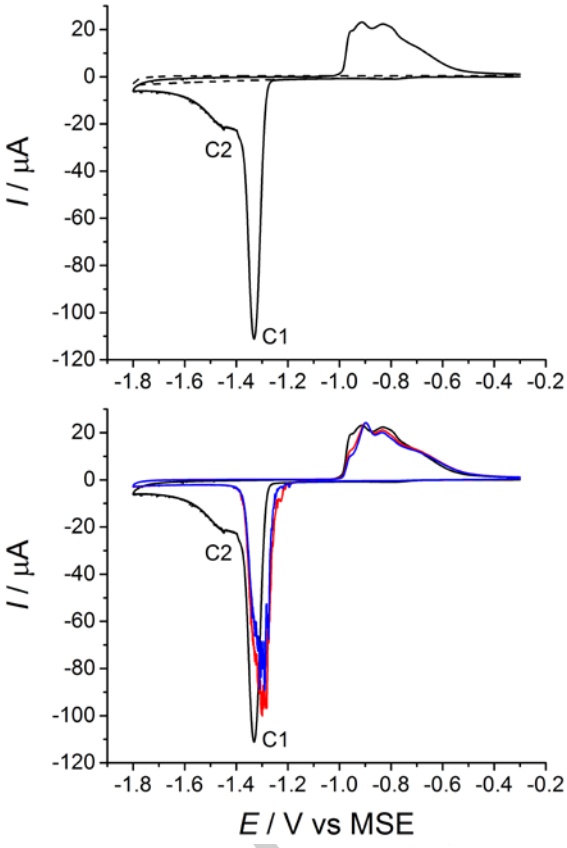

Figure 1. (Top) Cyclic stripping voltammetry in 0.10 M NaOH at 50mV s^{-1} (dashed line) bare GC (solid line) 0.69 nmoles of Bi_2O_3 NP modified GC. (Bottom) Consecutive scans of Bi_2O_3 modified GC (black) scan 1 (red) scan 2 (blue) scan 3.

The presence of the C2 process may indicate a OH^- deficiency within the drop-cast layer. This might be due to the prevalence of aggregates/agglomerates forming during drying and the inhibited diffusion of the electrolyte into the clusters[5b]. On the reverse scan a wide oxidation peak is observed. The process occurring here can be rationalised by considering the respective change in the oxidation and reduction peak in consecutive scans of the drop-cast NPs as seen in Fig 1 (bottom). Clearly the C2 process is not present after the first scan, consistent with OH^- produced during the reduction of Bi_2O_3 in the first scan and remaining in the diffusion layer of the electrode, allowing dominance of the C1 process. During the scans, the size of the oxidation peak remains approximately constant, with the only significant change being the size of the reduction peak between scan 1 and scan 2, with this ending up equating to that of the oxidation peak. This strongly indicates that the oxidation process occurring is dominated by the reverse of the $3e^-$ process C1.

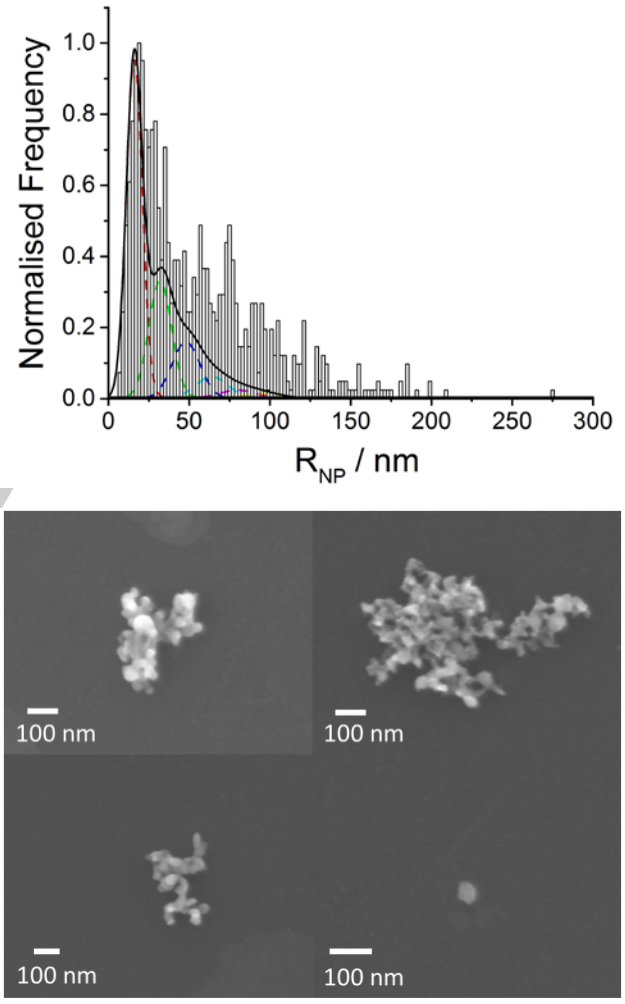

Figure 2. (Top) NP distribution as found from NTA, showing deviations from entropy only model[23]. (Bottom) SEM of drop-cast NPs showing Bi_2O_3 clusters and monomer.

Prior to nano-impact experiments the NP suspension was characterised by NTA as shown in Fig 2. A heavily agglomerated/aggregated system is observed, with a monomer radius of 19 nm, calculated from the peak modal value, matching the supplier specification of 19 nm. Sonication of the sample was found to have little impact on the distribution obtained indicating a fast rate of cluster formation of Bi_2O_3 NPs. Zeta potential measurements of the NPs in 0.10 M $NaNO_3$ showed the particles to have a zeta potential of -11 mV. The fitting shown in Fig 2. is that for the entropy only model[15] which has been shown to explain the agglomeration behaviour in capped metallic NPs. The achieved distribution in this case approximates the entropy only model with some larger particles present.

Next, nano-impact experiments were conducted on the agglomerated particles to study the agglomeration process. As there are two competing reductive processes occurring for Bi_2O_3 in the chose electrolyte, nano-impact experiments were conducted at a range of potentials from -1.1 V to -1.70 V vs MSE.

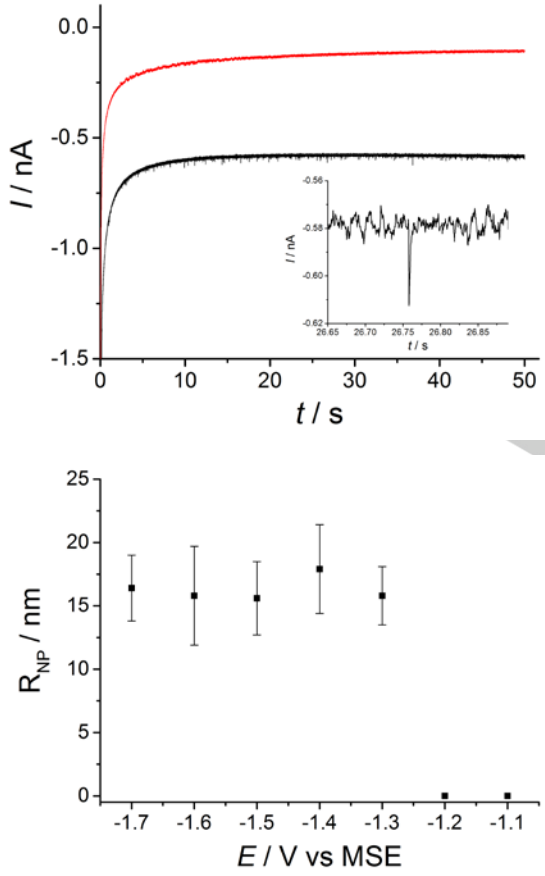

Figure 3. *(Top) Current-time transient at a CF microelectrode held at -1.70 V vs MSE in 0.10 M NaOH (red line) No NPs (black line) 40 pM Bi_2O_3 NPs. Increase in background current on addition of NPs attributed to reduction of small amounts of solubilised bismuth hydroxide species. Insert shows a zoomed in image of an example NP impact current trace. (Bottom) Average radius of NP as a function of held potential during current-time transient.*

Current-time transients were conducted at -1.70 V vs MSE with and without 40 pM NPs in 0.10 M NaOH. As seen in Fig 3 (top), current spikes were observed only when NPs were present indicating the reduction of Bi_2O_3 NPs. Experiments were conducted across the potential range mentioned and the size of the NPs calculated using the equation[6]:

$$R_{NP} = \sqrt[3]{\frac{3M_wQ}{4nF\pi\rho}}$$

where R_{NP} is the radius of the NP, M_w is the molecular weight of the composite material (465.96 $gmol^{-1}$), Q is the charge under the spike, n is the number of electrons involved in the reduction, F is Faraday's constant and ρ is the density of the material (9.17 gcm^{-3})[22]. Fig 3 (bottom) shows the resultant mean sizes of the NPs detected assuming the C1 process operates for which n=3. A clear potential dependence is observed, with no NPs being detected at potentials positive of -1.20 V vs MSE, concurrent with the stripping voltammetry in Fig 1. The consistent mean radius of the NPs from -1.30 V to -1.70 V vs MSE also suggests that the C2 process does not occur. This is to be expected as mass transport to an individually impacting NP is exceedingly fast[23] and would allow sufficient supply of OH^- to promote the $3e^-$ reduction.

As the NTA observed the presence of clusters, the size of the NPs detected by nano-impacts was studied as a function of time. Fig 4 (top) shows a plot of the average NP radius plotted against the start time of each 50 second current-time transient at -1.70 V vs MSE, with the first scan (T=0) occurring 2 minutes after NP addition to the electrolyte. No significant change in the average NP radius can be observed across the 20 minute time period, with the average NP radius remaining constant at approx. 17 nm. This suggests that the NPs detected by nano-impacts are confined to monomeric NPs only, with no NP clusters detected. To achieve a NP size distribution from nano-impact experiments, the resultant radii for the 851 spikes analysed across potentials from -1.30 V to -1.70 V vs MSE were combined as seen in Fig 4 (bottom). The mean radius of the NPs was found to be 17 nm with a standard deviation of 3 nm showing close agreement with that of the monomer found by NTA analysis and confirming the near exclusive detection of monomeric Bi_2O_3 NPs. This difference of 2 nm radius matches that calculated for the loss of material by formation of some soluble $Bi(OH)_x^{3-x}$ species. The amount of material lost was calculated using Medusa equilibrium software[24] at the concentrations and pH stated for nano-impacts experiments. This assumes equilibrium is reached prior to experimentation.

NTA analysis shows large proportions of clusters, which would be expected to be observed by impact voltammetry as estimated on the basis of their diffusion coefficients if they are present in the diffusion layer of the electrode[5b]. This observation is seemingly in contrast to that previously reported where agglomerates were detected in their clustered form[16]. The detection of only the Bi_2O_3 monomer by electrochemical methods suggests that Bi_2O_3 clusters *reversibly* agglomerate/deagglomerate much faster than the NP systems previous studied and may explain why only monomeric NPs are

detected where larger clusters are not observed even over extended time periods. Simply put the dimer, trimer and higher order agglomerated clusters which are slow diffusing dissociate within the diffusion layer so that the faster diffusing monomeric species are detected:

$$\mathrm{nmer} \rightleftharpoons (\mathrm{n}-1)\mathrm{mer} + \mathrm{monomer}$$
$$(\mathrm{n}-1)\mathrm{mer} \rightleftharpoons (\mathrm{n}-2)\mathrm{mer} + \mathrm{monomer}$$
$$\mathrm{trimer} \rightleftharpoons \mathrm{dimer} + \mathrm{monomer}$$
$$\mathrm{dimer} \rightleftharpoons \mathrm{monomer} + \mathrm{monomer}$$
$$\mathrm{monomer} + 6\mathrm{Ne}^- + 3\mathrm{H_2O} \rightarrow 2\mathrm{NBi}^{3+} + 6\mathrm{OH}^-$$

where N is the number of molecules of Bi_2O_3 present in a monomeric NP.

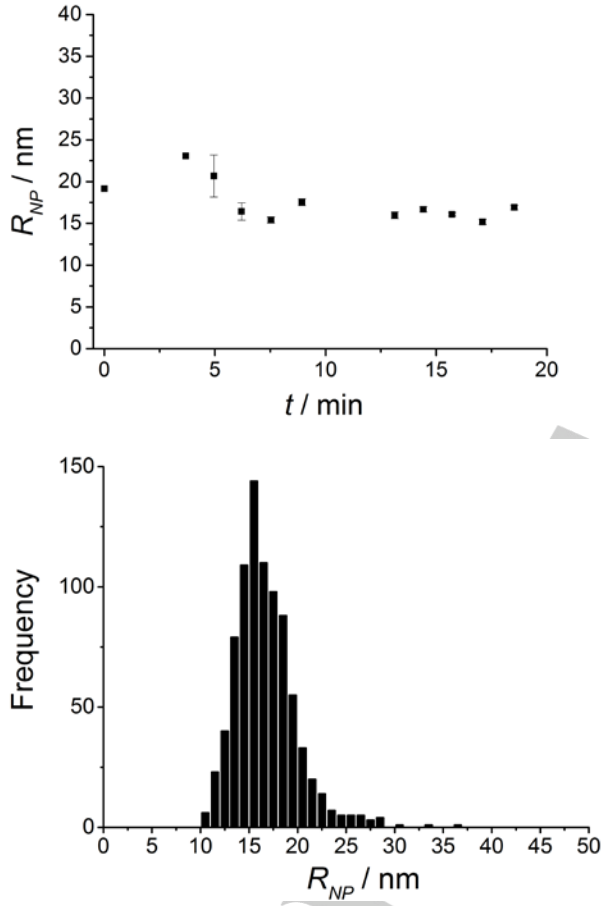

Figure 4. *(Top) Mean radius of NP vs start time of 50 second current-time transient. (Bottom) Size distribution of Bi_2O_3 NPs summarised across potentials from -1.20 V to -1.70 V vs MSE.*

Recent work on the formation of nanoelectrode arrays by nano-impacts has shown it is possible to electrolyse single impacting metal halide NPs to leave nano-deposits of the corresponding metal on the electrode surface[20]. The ability of Bi_2O_3 to be reduced to Bi was therefore exploited to allow SEM imaging of surfaces impacted by Bi_2O_3 NPs at -1.60 V vs MSE. Fig 5 (top) shows the resultant GC electrode is covered with nanoscale bismuth deposits. Sizing of these deposits is shown in Fig 5 (bottom) alongside the original NP size distribution obtained from nano-impact experiments. The mean size of the nano-deposits was found to be 14 nm with a standard deviation of 3 nm which is in good agreement with that calculated from the impact voltammetry. What is evident is the distinct lack of deposits resulting from the impact of NP clusters. This provides direct microscopic evidence for the "fast" *reversible* agglomeration mechanism as illustrated in Scheme 1. "Fast" *reversible* agglomeration of Bi_2O_3 to form clusters ensures a constant source of monomeric NPs in suspension. As these clusters approach the electrode, the monomers are electrochemically reduced. This in turn drives the equilibrium towards the release of monomers for clusters approaching the electrode surface, effectively providing voltammetric perturbation of the system and immediate detection. This leads to the selective electrochemical detection of the monomeric NP component of the clusters by electrolytic induced, "fast" *reversible* deagglomeration.

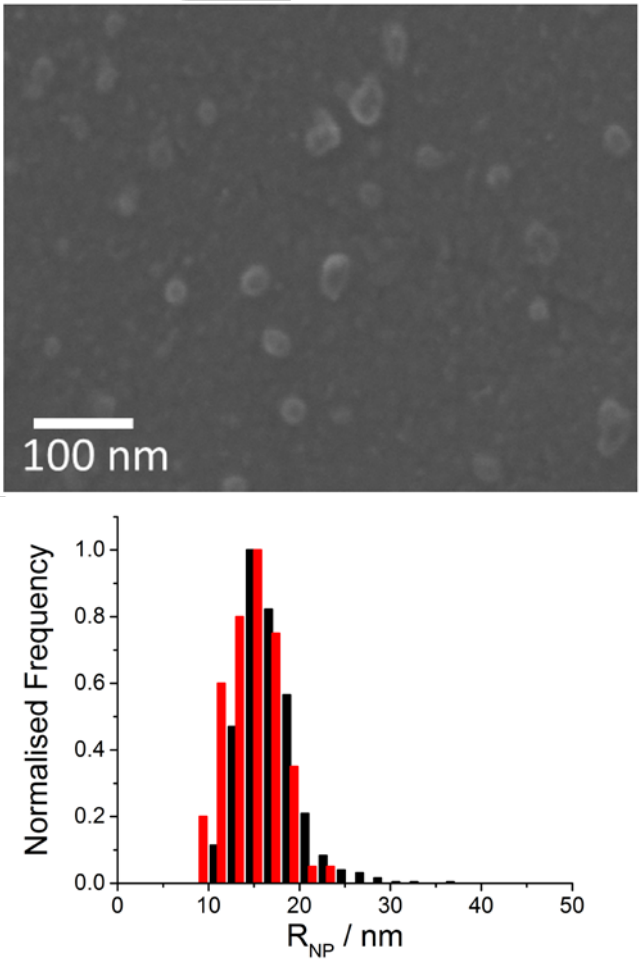

Figure 5. *(Top) SEM image of GC surface after 5 min deposition of Bi_2O_3 NPs at -1.60 V vs MSE in 40 pM Bi_2O_3 and 0.10 M NaOH. (Bottom) Comparison of size distributions obtained from (black) NP impacts (red) SEM of nano-deposits.*

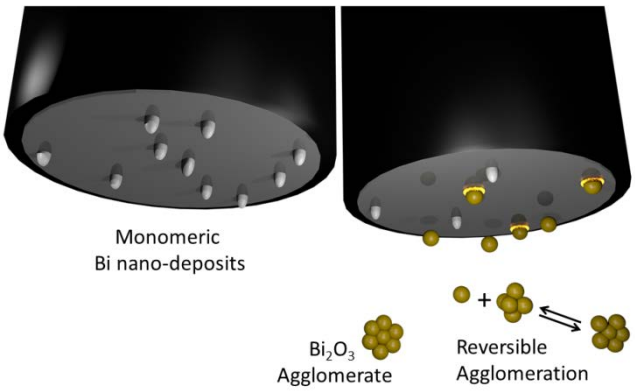

Scheme 1. *Reversible* agglomeration of Bi_2O_3 NPs approaching the electrode, resulting in the deposition of monomeric Bi nano-deposits.

Conclusions

The rapid agglomeration/deagglomeration of uncapped Bi_2O_3 clusters has been confirmed by voltammetric and microscopic study. By electrolytic detection of single NPs at the electrode surface, the *reversible* nature of agglomeration has been shown to promote the release of single NPs and provide selective detection of the monomer by nano-impacts. Voltammetric studies with Ag and Fe_3O_4 NPs have previously shown only slow agglomeration of NPs[16-18, 25], observable over experimental timescales, and the detection of dimeric, trimeric and higher ordered agglomerates as well as monomers. Here, NP suspensions consisting of entropically agglomerated clusters have been shown to undergo rapid deagglomeration to release monomers at an active electrode surface. The electrolysis of these monomers results in the deposition of metallic Bismuth onto the electrode surface. Direct microscopic evidence of pure monomer detection is provided by imaging of the electrode by SEM. By impacting the NPs the deposits are immobilised allowing imaging without drying induced agglomeration/aggregation effects. This is the first time the rapid agglomeration behaviour of metal oxide clusters has been studied by the nano-impact technique and provides a unique and complementary mode of study in conjunction with other analytical techniques.

Experimental Section

Chemicals

The NPs studied were 38 nm diameter NanoArc® bismuth oxide (Bi_2O_3, +99.5 %) nanopowder (Nanophase, USA). Sodium hydroxide (NaOH, ≥97 %) was supplied by Sigma Aldrich, UK. All dilutions used Millipore water with a resistivity of 18.2 MΩ.cm at 298 K.

Equipment

For electrochemical experiments the potentiostat used was an Autolab PGSTAT 302N (Metrohm-Autolab, Netherlands) fitted with an ECD module. All experiments were conducted in a thermostated Faraday cage held at 25 °C and solutions degassed with nitrogen. A three-electrode system was employed consisting of a saturated mercury sulphate reference electrode (MSE, equiv. to +0.64 V vs NHE) (BASi, UK), and a platinum wire counter electrode (Goodfellow Ltd, UK)[26].

Cyclic stripping voltammetry was conducted on a 3 mm diameter glassy carbon (GC) working macroelectrode (CH Instruments, USA). To modify the electrode, a known concentration of Bi_2O_3 NPs was suspended in H_2O by sonicating for 10 minutes and 5 µL dropped onto the electrode surface. This was dried under nitrogen to achieve a loading of 0.69 nmoles of Bi_2O_3.

For nano-impact experiments a 7 µm diameter carbon fibre (CF) working microelectrode, sealed in glass was used (BASi). NPs were suspended in water and sonicated for 10 minutes prior to addition to the NaOH electrolyte. After addition, bubbling with nitrogen was continued for 2 minutes to ensure thorough mixing of the NPs before electrochemical investigation. All electrodes were polished before use with 1, 0.3 and 0.05 µm alumina powder acquired from Buehler, UK.

Nanoparticle Characterisation

Nanoparticle tracking analysis (NTA) was used to provide solution phase characterisation of the NPs. A Nanosight LM10 (Nanosight, UK) was used and equipped with a sample chamber with a 638 nm laser. All measurements were conducted at room temperature and measured for a duration of 60 seconds at a frame rate of 30 frames per second. NTA 2.3 software was used for data capture. The sample preparation method was that previously used for nano-impact experiments and was conducted with a NP concentration of 40 pM for direct comparison with electrochemical experiments. Zeta potential measurements of the Bi_2O_3 NPs was conducted in 0.10 M NaOH with a NP concentration of 40 pM to allow direct comparison with voltammetric impact experiments. This was performed on a Zetasizer (Malvern, UK). Scanning electron microscopy (SEM) images of the NPs were taken using a JeoL JSM-6500F field SEM at 5 keV. Images of the drop-cast were carried out by modification of a GC sheet. For images of the Bi nano-deposits, nano-impact experiments were conducted with the GC sheet as the working electrode prior to imaging.

Acknowledgements

We acknowledge funding from the European Research Council (ERC) under the European Union's Seventh Frame-work Program (FP/2007-2013)/ERC Grant Agreement no. [320403].

Keywords: nano-impact • bismuth oxide • agglomeration • voltammetry • nanoparticle

[1] a) N. V. Rees, *Electrochem. Commun.* **2014**, *43*, 83-86; b) M. Pumera, *ACS Nano* **2014**, *8*, 7555-7558.
[2] Y. G. Zhou, N. V. Rees, R. G. Compton, *Angew. Chem., Int. Ed. Engl.* **2011**, *50*, 4219-4221.
[3] a) C. S. Lim, S. M. Tan, Z. Sofer, M. Pumera, *ACS Nano* **2015**, *9*, 8474-8483; b) D. Qiu, S. Wang, Y. Zheng, Z. Deng, *Nanotechnology* **2013**, *24*, 505707; c) B. Haddou, N. V. Rees, R. G. Compton, *Phys. Chem. Chem. Phys.* **2012**, *14*, 13612-13617; d) L. R. Holt, B. J. Plowman, N. P. Young, K. Tschulik, R. G. Compton, *Angew. Chem., Int. Ed. Engl.* **2016**, *55*, 397-400.

[4] K. Tschulik, B. Haddou, D. Omanović, N. V. Rees, R. G. Compton, *Nano Res.* **2013**, *6*, 836-841.
[5] a) T. R. Bartlett, C. Batchelor-McAuley, K. Tschulik, K. Jurkschat, R. G. Compton, *ChemElectroChem* **2015**, *2*, 522-528; b) T. R. Bartlett, S. V. Sokolov, R. G. Compton, *ChemistryOpen* **2015**, *4*, 600-605.
[6] W. Cheng, X. F. Zhou, R. G. Compton, *Angew. Chem., Int. Ed. Engl.* **2013**, *52*, 12980-12982.
[7] X. F. Zhou, W. Cheng, C. Batchelor-Mcauley, K. Tschulik, R. G. Compton, *Electroanalysis* **2014**, *26*, 248-253.
[8] W. Cheng, R. G. Compton, *Angew. Chem., Int. Ed. Engl.* **2014**, *53*, 13928-13930.
[9] L. Sepunaru, K. Tschulik, C. Batchelor-McAuley, R. Gavish, R. G. Compton, *Biomater. Sci.* **2015**, *3*, 816-820.
[10] L. Sepunaru, B. J. Plowman, S. V. Sokolov, N. P. Young, R. G. Compton, *Chem. Sci.* **2016**.
[11] a) L. V. Stebounova, E. Guio, V. H. Grassian, *J. Nanopart. Res.* **2010**, *13*, 233-244; b) D. J. Srolovitz, M. G. Goldiner, *JOM* **1995**, *47*, 31-36.
[12] a) C. Levard, E. M. Hotze, G. V. Lowry, G. E. Brown, Jr., *Environ. Sci. Technol.* **2012**, *46*, 6900-6914; b) P. J. Vikesland, A. M. Heathcock, R. L. Rebodos, K. E. Makus, *Environ. Sci. Technol.* **2007**, *41*, 5277-5283.
[13] a) S. Elzey, V. H. Grassian, *J. Nanopart. Res.* **2009**, *12*, 1945-1958; b) E. M. Hotze, T. Phenrat, G. V. Lowry, *J. Environ. Qual.* **2010**, *39*, 1909.
[14] J. V. Alemán, A. V. Chadwick, J. He, M. Hess, K. Horie, R. G. Jones, P. Kratochvíl, I. Meisel, I. Mita, G. Moad, S. Penczek, R. F. T. Stepto, *Pure Appl. Chem.* **2007**, *79*.
[15] S. V. Sokolov, E. Kätelhön, R. G. Compton, *J. Phys. Chem. C.* **2015**, *119*, 25093-25099.
[16] J. Ellison, K. Tschulik, E. J. Stuart, K. Jurkschat, D. Omanovic, M. Uhlemann, A. Crossley, R. G. Compton, *ChemistryOpen* **2013**, *2*, 69-75.
[17] S. V. Sokolov, K. Tschulik, C. Batchelor-McAuley, K. Jurkschat, R. G. Compton, *Anal. Chem.* **2015**, *87*, 10033-10039.
[18] K. Tschulik, R. G. Compton, *Phys. Chem. Chem. Phys.* **2014**, *16*, 13909-13913.
[19] a) D. Zhou, S. W. Bennett, A. A. Keller, *PLoS One* **2012**, *7*, e37363; b) A. Teleki, R. Wengeler, L. Wengeler, H. Nirschl, S. E. Pratsinis, *Powder Technol.* **2008**, *181*, 292-300.
[20] T. R. Bartlett, J. Holter, N. Young, R. G. Compton, *Nanoscale* **2016**, in press DOI: 10.1016/j.electacta.2016.02.031.
[21] a) A. M. Espinosa, M. T. San José, M. L. Tascón, M. D. Vászquez, P. Sánchez Batanero, *Electrochim. Acta* **1991**, *36*, 1561-1571; b) G. H. Hwang, W. K. Han, S. J. Kim, S. J. Hong, J. S. Park, H. J. Park, S. G. Kang, *J Ceram Process Res* **2009**, *10*, 190-194.
[22] S. K. Blower, C. Greaves, *Acta Crystallogr., Sect. C: Cryst. Struct. Commun.* **1988**, *44*, 587-589.
[23] J. M. Kahk, N. V. Rees, J. Pillay, R. Tshikhudo, S. Vilakazi, R. G. Compton, *Nano Today* **2012**, 7, 174-179.
[24] I. Puigdomenech, MEDUSA, avaliable from; https://www.kth.se/en/che/medusa/downloads-1.386254.
[25] N. V. Rees, Y. G. Zhou, R. G. Compton, *ChemPhysChem* **2011**, *12*, 1645-1647.
[26] E. Kätelhön, E. E. L. Tanner, C. Batchelor-McAuley, R. G. Compton, *Electrochim. Acta.* **2016**, in press DOI: 10.1016/j.electacta.2016.02.031.

Entry for the Table of Contents (Please choose one layout)

Layout 1:

FULL PAPER

Reversible agglomeration of uncapped Bi_2O_3 nanoparticles is revealed by nano-impacts, nanoparticle tracking analysis and microscopic imaging. A minimum rate for the deagglomeration/agglomeration of the particles is estimated.

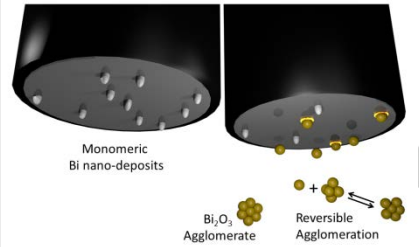

*Author(s), Corresponding Author(s)**

Page No. – Page No.

Title